β-Amyloid Induces Paired Helical Filament-like Tau Filaments in Tissue Culture*

Alessandra Ferrari‡§, Frederic Hoerndli‡, Thomas Baechi¶, Roger M. Nitsch‡, and Jürgen Götz‡‖

From the ‡Division of Psychiatry Research, University of Zürich, August Forel Strasse 1, 8008 Zürich and the ¶Central Laboratory for Electron Microscopy, University of Zurich, Gloriastrasse 30, 8028 Zurich, Switzerland

Paired helical filaments (PHF) are the principal pathologic components of neurofibrillary tangles in Alzheimer's disease (AD). To reproduce the formation of PHF in tissue culture, we stably expressed human tau with and without pathogenic mutations in human SH-SY5Y cells and exposed them for 5 days to aggregated synthetic β-amyloid peptide ($A\beta_{42}$). This caused a decreased solubility of tau along with the generation of PHF-like tau-containing filaments. These were 20 nm wide and had periodicities of 130–140 nm in the presence of P301L mutant tau or 150–160 nm in the presence of wild-type tau. Mutagenesis of the phosphoepitope serine 422 of tau prevented both the $A\beta_{42}$-mediated decrease in solubility and the generation of PHF-like filaments, suggesting a role of serine 422 or its phosphorylation in tau filament formation. Together, our data underscore a role of $A\beta_{42}$ in the formation of PHF-like filaments. Our culture system will be useful to map phosphoepitopes of tau involved in PHF formation and to identify and characterize modifiers of the tau pathology. Further adaptation of the system may allow the screening and validation of compounds designed to prevent PHF formation.

Neurofibrillary tangles (NFT)[1] are abundant in many neurodegenerative diseases, including Alzheimer's disease (AD) and frontotemporal dementia with Parkinsonism linked to chromosome 17 (FTDP-17) caused by mutations in the *tau* gene (1–3). NFT are composed of filamentous aggregates that include paired helical filaments (PHF) and narrow twisted ribbons. These are made of the microtubule-associated protein tau (4, 5). Tau in these filaments is hyperphosphorylated both at physiological sites and at additional, pathological sites. Phosphorylation of tau is associated with the dissociation of tau from microtubules and with its relocalization from axons to cell

bodies and dendrites. Pathologic increases in this pool of soluble tau, along with conformational changes of the natively unfolded tau, are initial critical steps in the assembly of the more insoluble pathological tau filaments.

Transgenic mice expressing pathogenic mutations of human tau generate a few low abundant NFT (6, 7), and both intracerebral microinjections of β-amyloid into P301L mutant tau transgenic mice and co-expression of mutant amyloid precursor protein greatly accelerate the rate of NFT formation in mice (8, 9). These data established a mechanistic relationship of β-amyloid toxicity with NFT formation.

To circumvent the inherent limitations of the above *in vivo* experiments (including poor breeding of doubly transgenic mice as well as stereotaxic techniques) and to establish PHF formation in tissue culture, we expressed both wild-type and mutant forms of human tau in human SH-SY5Y cells and exposed them to preparations of aggregated synthetic β-amyloid. We were able to produce *bona fide* PHF-like tau filaments within 5 days of tissue culture.

EXPERIMENTAL PROCEDURES

Site-directed Mutagenesis—The longest human 4-repeat tau isoform, htau40, was cloned into the pRc/RSV expression vector (Invitrogen). Site-directed mutagenesis (QuikChange kit; Stratagene) was performed to generate the tau mutant P301L and the double mutants, P301L/S422E and P301L/S422A. The sequences of the mutagenized oligonucleotides were as follows: P301L, 5′-GGTTTGTAGACTATTTGCAC-ACTGCCGCCTCCCTGGACGTGTTTG-3′; S422E, 5′-GCATCGACAT-GGTAGACGAGCCCCAGCTCGCCACGC-3′; S422A, 5′-GCATCGA-CATGGTAGACGCGCCCCAGCTCGCCACGC-3′. All constructs were sequenced to confirm the absence of randomly introduced mutations.

Cell Culture—Human SH-SY5Y neuroblastoma cells were transfected with either wild-type or mutant htau40 cDNA constructs using LipofectAMINE 2000 (Invitrogen) and selected with 125 μg/ml G418 for 30 days. Pools of selected clones were seeded at a density of $0.3–2.0 \times 10^4$ cells/cm², depending on the type of experiment (low density culture for immunocytochemistry and high density culture for electron microscopy and Western blot analysis). To normalize for cell numbers, undifferentiated cells were seeded at a density which, after $A\beta_{42}$ incubation for 5 days, was below 50% and thus comparable with numbers of differentiated cells at the time of $A\beta_{42}$ treatment. To induce neuronal differentiation, cells were seeded on collagen type I-coated dishes and treated with 20 μM all-*trans*-retinoic acid (Sigma) for 5 days in standard culture medium and cultivated for an additional 5 days in serum-free medium complemented with 50 ng/ml brain-derived neurotrophic factor (Peprotech, Lucerne, Switzerland) (10).

Neuronal properties were confirmed by the presence of neuronal markers and the absence of glial markers (data not shown). Moreover, the cells expressed synaptophysin when cultured on murine organotypic hippocampal slices.[2] Two independent lots of $A\beta_{42}$ (Nos. 524548 and 535120) and $A\beta_{42-1}$ (Lot No. 536763) were synthesized by Bachem (Bubendorf, Switzerland), reconstituted in PBS at calculated concentrations of 220 μM, shaken at 1000 rpm for 24 h at 37 °C, and analyzed by electron microscopy. This preparation contained β-amyloid fibrils

---

§ Present address: Medical Research Council Laboratory for Molecular Cell Biology, University College of London, Gower St., London WC1E 6BT, United Kingdom.

‖ To whom correspondence should be addressed: Division of Psychiatry Research, University of Zürich, August Forel Str. 1, 8008 Zürich, Switzerland. Tel: 41-1-634-8873; Fax: 41-1-634-8874; E-mail: goetz@bli.unizh.ch.

[1] The abbreviations used are: NFT, neurofibrillary tangles; AD, Alzheimer's disease; PHF, paired helical filaments; PBS, phosphate-buffered saline; FA, formic acid; IC, immunocytochemistry; ELISA, enzyme-linked immunosorbent assay.

[2] O. Raineteau and A. Ferrari, data not shown.

along with protofibrils and SDS-stable oligomers (11). Suspensions of Aβ$_{42}$ preparations corresponding to 10 μM soluble peptide were added to each culture for 1–5 days for immunohistochemistry or 2–5 days for sarkosyl extractions and electron microscopy. Once Aβ$_{42}$ preparations had been added to the cells, the medium was not changed. This, in addition to the stickiness of Aβ$_{42}$, may explain why Aβ$_{42}$ formed large clumps on the cells as visualized by immunocytochemistry and electron microscopy. Lactate dehydrogenase assays (Sigma) were performed to measure the toxicity of Aβ$_{42}$.

Immunofluorescence Analysis and Antibodies—For immunocyto-chemistry, cells were grown on collagen-coated coverslips and fixed with 4% paraformaldehyde in microtubule-stabilizing buffer at room temperature for 30 min, followed by permeabilization with 0.3% Triton X-100. The following antibodies were used for immunocytochemistry (IC), Western blotting (WB), and electron microscopy (EM): HT7 (Inno-genetics Inc, Belgium; amino acids 159–163; IC, 1:300; WB, 1:300) and Tau-5A6 (Developmental Studies Hybridoma Bank; EM, 1:50) (12) were used to specifically detect human tau. Antisera Ser422P 988 (Dr. Andre Delacourte; IC: 1:1000) (13), and pS422 (BIOSOURCE Inc., Nivelles, Belgium; IC, 1:1000) were used to detect tau phosphorylated at Ser-422. Antibodies for neuronal markers included NF200 (Sigma; IH, 1:400), NSE (Dako, Glostrup, Denmark; IC, 1:200), and MAP2 (Chemicon, Temecula, CA; IC, 1:400), and as a glial marker GFAP (Sigma; IC, 1:100) was used. Monoclonal antibody 4G8 (Signet Laboratories, Ded-ham, MA; IC, 1:500; EM, 1:50) was used to detect Aβ amyloid peptide. Secondary antibodies for immunofluorescence were obtained from Jack-son Laboratories (West Grove, PA). For a quantification, two independent experiments were performed and 200 cells were counted for each experimental condition.

Western Blot Analysis, Aβ-ELISA, and Quantitative RT-PCR—Tau-expressing cells were grown on 10-cm dishes and extracted in RIPA buffer as described previously (14). Proteins were separated on a 10% NuPAGE gel (Invitrogen), blotted onto a nitrocellulose membrane, and probed with HT7 and a β-actin-specific antibody (Abcam, Cambridge, UK; 1:5000).

The levels and solubility of tau protein were determined by extracting Aβ-treated and control cells using buffers with increasing ionic strengths (14). The cells were homogenized in high-salt reassembly (RAB) buffer to generate the RAB-insoluble fractions. Following centrifugation, the pellets were homogenized in RIPA buffer and centrifuged. The RIPA-insoluble pellets were extracted with 70% formic acid (FA) to give the FA fractions. Centrifugation was done at 50,000 × g for 20 min. Protein concentrations of the samples from each fraction were adjusted to equal levels and the same amounts of protein run on a 10% NUPAGE gel and blotted as described above. As loading control and to exclude contamination of the FA fraction with soluble proteins, the blots were probed with a GAPDH-specific monoclonal antibody (BioDe-sign, Saco, ME; 1:500). Furthermore, an Aβ$_{42}$-specific ELISA (Innoge-netics, Gent, Belgium) was included for a subset of the samples.

For quantification, the Western blots were probed with the tau-specific antibody HT7 and analyzed by densitometry. The same exposure time was chosen for all blots. The x-ray films were scanned at 400 ppi and the images analyzed with the AlphaEase software (Alpha Innotech Corp., San Leandro, CA). For the purpose of graphic representation, for each blot the intensity values of all time points were normalized using the value at time point t 0. Statistical analysis of the intensity differences between PBS- and Aβ$_{42}$-treated samples was done with the original intensity values, because only the relative and not the absolute differences are relevant for the two-tailed Student's t test.

The real-time quantitative PCR for tau was done with HPLC-purified primers and an HPLC-purified probe (forward primer, 5′-CAA-GACCAAGAGGGTGACACG-3′; reverse primer, 5′-TCAGAGCCCGGT-TCCTCAG-3′ (Metabion GmbH, Martinsried, Germany); TaqMan probe, 5′-6-FAM-CTGGCCTGAAAGAATCTCCCCTGCA-BHQ-1-3′ (Biosearch Technologies Inc., Novato, CA). As reference gene, the Taq-Man rodent *GAPDH* control no. 4308313 (Applied Biosystems, PerkinElmer Life Sciences) was used and ΔCt values (cycle threshold values) were determined.

Sarkosyl Extraction and Immunoelectron Microscopy—Sarkosyl extractions of tau were done as previously described (15). The extracts were placed on formvar/carbon-coated 300-mesh grids and incubated with the primary antibody in PBS/0.1% gelatin for 90 min at room temperature. Antibody Tau-5A6 was used at a 1:50 dilution. As a positive control, AD brain extracts were included; the secondary antibody used for AD extracts was either conjugated to gold (data not shown) or not (for Fig. 4). In addition, extracts were incubated with the Aβ$_{42}$-specific antibody 4G8 at 1:50 dilutions. Again, controls were included in which the primary antibody had been omitted. Grids were

incubated with 6 nm Au-conjugated or unconjugated secondary anti-bodies (Aurion, Wageningen, Netherlands) and stained with 2% phos-photungstic acid. Micrographs were recorded on a Philips model CM12 electron microscope.

Thin Section Immunoelectron Microscopy—To visualize β-amyloid on the cells, samples were fixed in 4% paraformaldehyde and 0.1% glut-araldehyde. Following fixation, tissue blocks were epoxy-embedded, sectioned with a Reichert Ultracut E microtome (Leica, Solms, Germa-ny), placed on 200-mesh copper grids, and stained with uranyl acetate and lead citrate. To visualize tau filaments, cells were fixed in 3% paraformaldehyde and 0.1% glutaraldehyde for 30 min at room tem-perature, washed with 50 mM NH$_4$Cl in PBS, embedded in 3% agar (Noble; Difco Laboratories, Detroit, MI), and submerged in sucrose-PVP 2 M (Sigma) for 3 days. Samples were mounted and cut on a Reichert Ultracut S cryostat (Leica) to obtain ultra-thin sections. Grids were processed for immunolabeling as follows. After a blocking step in 5% goat serum in PBS for 20 min, the primary anti-tau antibody Tau-5A6 was added in 1% goat serum in PBS at a 1:50 dilution for 2 h, followed by a 6-nm gold-coupled goat anti-mouse antiserum (Aurion) in 1% bovine serum albumin in PBS at a 1:5 dilution for 1 h. Controls were included in which the primary antibody had been omitted. Washes were done with 1% bovine serum albumin in PBS for 10 min. Finally, the grids were stained with 3% uranyl acetate and 2% methylcellulose. Micrographs were recorded on a Philips model CM12 electron micro-scope. To determine the number of gold-decorated tau filamentous aggregates/cell, a cut-off of 15 gold particles per aggregate was defined, and groups of gold particles were counted per cell in 30 Aβ$_{42}$-treated compared with 30 untreated cells.

<div align="center">RESULTS</div>

Aβ$_{42}$ Decreases the Solubility of Tau—To assess the role of Aβ$_{42}$ in tau aggregation and filament formation in tissue cul-ture, we added preparations of aggregated synthetic Aβ$_{42}$ to the media of SH-SY5Y cells that had been stably transfected with expression constructs encoding the longest 4-repeat iso-form of human tau, with or without the pathogenic FTDP-17 mutation P301L (Fig. 1*A*). Confocal analysis confirmed the presence of Aβ$_{42}$ aggregates deposited on both cell bodies and neurites (Fig. 1*B*). Neither the size nor the number of these aggregates varied within 1 and 5 days of incubation. Electron-microscopic analyses demonstrated that Aβ$_{42}$ aggregates con-tained the expected amorphous fibrous material that was sim-ilar to that extracted from brain β-amyloid plaques (Fig. 1, *C–E*). In this assay system the initial 5 days of treatment with Aβ$_{42}$ were not accompanied by any obvious increases in cell death, and lactate dehydrogenase (LDH) assays did not reveal increased LDH release, as compared with vehicle controls (data not shown).

Western blots confirmed that cellular levels of human tau were similar in all transfected conditions, both in undifferen-tiated cells (data not shown) and cells that were sequentially differentiated with retinoic acid and brain-derived neurotro-phic factor (Fig. 1*A*).

To determine the role of Aβ$_{42}$ in the aggregation of tau, we used undifferentiated cells that expressed wild-type human tau. We extracted cellular proteins in high-salt RAB buffer to generate the RAB fraction. We then homogenized the RAB-insoluble pellet in RIPA buffer to obtain RIPA-soluble proteins and extracted the RIPA-insoluble pellet with FA to obtain the FA-soluble protein fraction (Fig. 2). Equal amounts of total protein of the treated and untreated fractions were loaded, but the FA fractions contained less protein than the RAB and RIPA fractions. The signals in the three fractions could not be added up to determine the total amount of tau, because tau had been sequentially extracted. After 1 day of Aβ$_{42}$ treatment, most tau was present in the RAB fraction and only a small fraction was RAB-insoluble and found in the RIPA fraction, as compared with none in the RIPA fraction of the vehicle-treated cells (Fig. 2*A*). During 5 days of incubation with Aβ$_{42}$, the solubility of tau decreased significantly because a substantial amount of it ap-peared in the RIPA and FA fractions. In contrast, in untreated
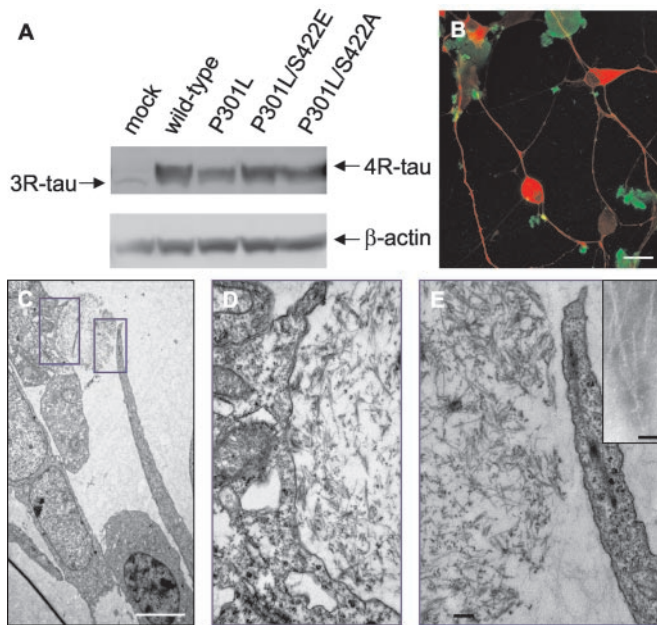
FIG. 1. **Aβ$_{42}$ aggregates are deposited on tau-expressing cells.** *A*, Western blot analysis of neuronally differentiated cells using a human tau-specific antibody reveals comparable levels of transfected 4-repeat tau in wild-type, P301L, P301L/S422E, and P301L/S422A cells (*arrow*). Undifferentiated cells express comparable levels of 4-repeat tau (data not shown). Levels of 4-repeat tau are more than 10-fold increased when compared with endogenous 3-repeat tau in the mock-transfected control cells (*arrow*). β-Actin staining is included to confirm equal loading. *B*, confocal analysis of cells shows that Aβ$_{42}$ (4G8, *green*) forms large clumps on the cell bodies and processes of neuronally differentiated tau-expressing cells (HT7, *red*). Intracellular accumulation of Aβ$_{42}$ is not detectable. *C*, electron microscopy of an Aβ$_{42}$ deposit in contact with a cell (low magnification) illustrates the filamentous structure of Aβ$_{42}$ in the two *boxed areas* shown at higher magnification in *panels D* and *E*. The *inset* in *panel E* shows sarkosyl-extracted Aβ$_{42}$ fibrils that are 7–10 nm wide and lack regular periodicities. *Scale bar*, 20 μm (*B*), 3 μm (*C*), and 40 nm (*panel E, inset*).

control cells, tau was absent from the FA fraction after 5 days of incubation with the vehicle (Fig. 2*B*). In addition to full-length tau, we observed, at variable degrees, truncated tau with a molecular mass of 28 kDa. Probing of the blots (Fig. 2*B*) with a GAPDH-specific monoclonal antibody confirmed equal amounts of protein in the RAB fraction. Moreover, we could exclude a carryover of soluble proteins into the FA fraction (Fig. 2*C*). An Aβ$_{42}$-specific ELISA (Innogenetics) was included for a subset of the samples. This assay showed that substantial amounts of Aβ$_{42}$ were in the RIPA and FA fraction (data not shown). Therefore, by loading equal amounts of protein of the Aβ$_{42}$- and PBS-treated FA fractions, the amount of FA-soluble tau is likely to be underestimated in the Aβ$_{42}$-treated compared with the PBS-treated FA fractions. Next, to monitor the kinetics of tau assembly, combined levels of FA-soluble full-length and truncated tau were quantified after incubation with Aβ$_{42}$ for 0 h, 6 h, 1 d, 3 d, and 5 d and compared with PBS-treated controls. Three independent experiments revealed an increase of tau in the FA fraction with longer exposure to Aβ$_{42}$ that was statistically significant at 5 d (Fig. 2*D*, *, two-tailed Student's *t* test; *p* = 0.03).

To determine whether Aβ$_{42}$ affects tau transcription, we performed a quantitative RT-PCR analysis. When undifferentiated P301L cells were compared with mock-transfected cells at time point 0, we found that incubation with Aβ$_{42}$ for 5 days did not alter tau mRNA levels, either in mock- or P301L-transfected cells (Fig. 3).

Aβ$_{42}$ Induces PHF-like Tau Filaments—To determine whether the decreased solubility of tau in response to exposure
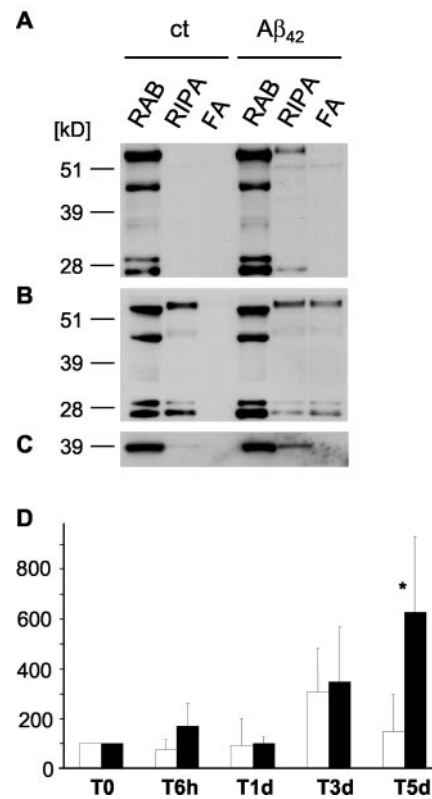

FIG. 2. **Solubility of tau in transfected SH-SY5Y cells.** *A*, sequential extraction of both untreated and Aβ$_{42}$-treated undifferentiated wild-type tau-expressing cells in high-salt RAB buffer, RIPA buffer, and FA already reveals after a 1-day incubation with Aβ$_{42}$ a small fraction of tau in the RIPA fraction, in contrast to untreated cells. *B*, after a 5-day incubation with Aβ$_{42}$ the solubility of tau is significantly decreased as a substantial fraction of tau is present in both the RIPA and FA fractions, whereas in untreated cells after a 5-day culture period, tau is present in the RIPA fraction but absent in the FA fraction. *C*, as loading control, GAPDH (39 kDa) has been included. *D*, to monitor the kinetics of tau insolubility, tau in the FA fraction is shown after incubation with PBS (□) or Aβ$_{42}$ (■) for 0 h, 6 h, 1 d, 3 d, and 5 d. For each experiment, the ratio of the intensities for each time point was determined relative to the value at time point *t* 0. Intensity values are given in percentages. The data represent the mean of three independent experiments for time points *t* 6 h, 1 d, and 5 d, and two for *t* 3 d. A two-tailed Student's *t* test reveals statistically significant differences (*, *p* = 0.03) after 5 days of incubation with Aβ$_{42}$.

to Aβ$_{42}$ was associated with the formation of PHF, we analyzed sarkosyl protein extracts by negative contrast electron microscopy (Fig. 4). As a control, we included sarkosyl extracts from a human brain with a confirmed NFT pathology. It contained many PHF with expected widths of 20 nm and periodicities of 75–80 nm (Fig. 4*A*) (16).

Immunoelectron microscopy of sarkosyl protein extracts of undifferentiated SH-SY5Y cells expressing wild-type human tau with the monoclonal antibody Tau-5A6 identified many twisted filaments with widths of up to 20 nm, periodicities of 150–160 nm, and lengths of up to 1200 nm (Fig. 4, *B* and *C* and Table I). They resembled the PHF extracted from NFT in human neurodegenerative diseases and are best described as narrow twisted ribbons (17).

Because the ultrastructural characteristics of abnormal filaments in human neurodegenerative diseases vary with pathogenic mutations (4, 5), we analyzed the abnormal filaments generated by P301L mutant tau. Again, Aβ$_{42}$ caused the generation of PHF-like filaments both in differentiated and undifferentiated cells stably transfected with P301L mutant tau (Fig. 4, *D* and *E* and Table I). These PHF had shorter periodicities of 130–140 nm with similar widths as compared with the
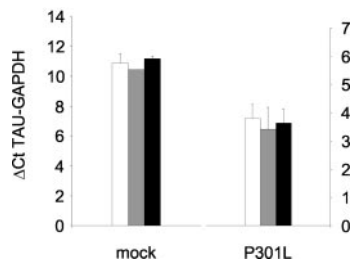
FIG. 3. **Aβ$_{42}$ does not cause increased transcription of tau mRNA.** After incubation with PBS for 5 days (*gray*), slight increases of tau mRNA levels (as shown by Δ*Ct* (cycle threshold) values for tau compared with the reference gene *GAPDH*) are found for both mock- and P301L-transfected cells, compared with time point *t* 0 (*white*). These are statistically not significant (two-tailed Student's *t* test; *p* > 0.38). After incubation with Aβ$_{42}$ for 5 days (*black*), levels are slightly decreased in both cell types. These differences are again not statistically significant (two-tailed Student's *t* test; *p* > 0.14), demonstrating that Aβ$_{42}$ does not cause increased tau transcription. In addition, this analysis reveals ~60-fold higher tau mRNA levels in P301L compared with mock-transfected cells (as shown by the lower Δ*Ct* values).

wild-type tau filaments, consistent with the fact that mutations can affect the phenotype of the tau filaments.

To exclude that the PHF-like filaments contained β-amyloid fibrils derived from our Aβ$_{42}$ preparation, we showed that the anti-Aβ$_{42}$ antibody 4G8 failed to decorate the PHF, whereas it clearly decorated β-amyloid fibrils extracted with the identical sarkosyl protocol (data not shown). Moreover, we found with electron microscopy that our β-amyloid fibrils were 7–10 nm wide and lacked regular periodicities (Fig. 1*E*, *inset*) (11). Control experiments showed that neither vehicle controls nor identical preparations of the reverse peptide Aβ$_{42–1}$ caused the formation of PHF.

Neuronally differentiated SH-SY5Y cells transfected with either wild-type or P301L tau also formed many PHF-like filaments after 5 days of exposure to the Aβ$_{42}$ preparation (Table I). This may be because of similar cellular levels of human tau in both differentiated and undifferentiated cells, in that cellular levels of tau in the transfected cells exceeded those of endogenous 3-repeat tau (18) by more than 10 times (Fig. 1*A*).

A quantitative analysis of filament formation in sarkosyl extracts by negative staining electron microscopy is impossible because the adherence of the sample to the grid surface is irregular, due to the irreproducibility of the surface charge of the carbon-coated grids. Thus, filaments may cluster in one field of a grid, whereas another field may be completely empty.

A semi-quantitative analysis can be achieved by immunoelectron microscopy on ultra-thin cryosections of cells. We treated undifferentiated wild-type tau-expressing cells either with Aβ$_{42}$ or PBS and obtained cryosections that were incubated with the human tau-specific antibody Tau-5A6, followed by a gold-labeled secondary antibody. As a control, the primary antibody was omitted. Cryoelectron microscopy has the disadvantage that cellular structures are not resolved, but antibodies can penetrate the sections more easily. Many gold-decorated aggregates were revealed in the cytoplasm of neurons that were treated with Aβ$_{42}$ (Fig. 5, *A* and *B*). For a quantification, an arbitrary cut-off of 15 gold particles was defined to increase the stringency and to reduce the background. Groups of gold particles were counted per cell in Aβ$_{42}$-treated compared with untreated cells. This revealed a strong increase in the number of tau aggregates in Aβ$_{42}$-treated cells (Fig. 5*C*).

Role of Epitope Ser-422 of Tau in Aggregation and Filament Formation—In transgenic mice expressing P301L tau, Ser-422 was among the epitopes that were selectively phosphorylated in response to Aβ$_{42}$ injections (9). Therefore, we stained both
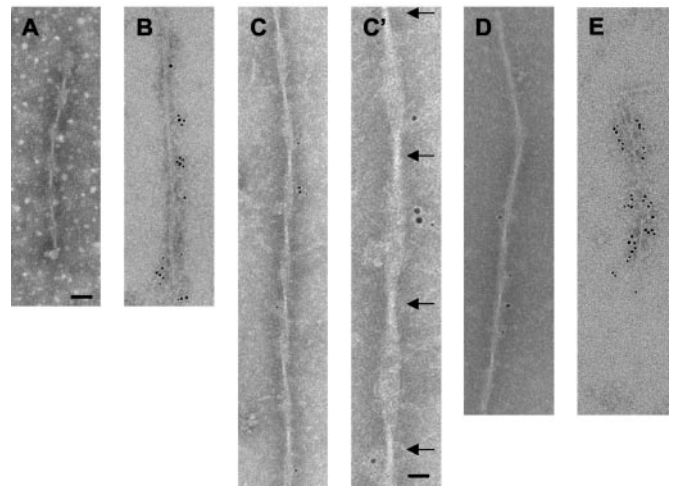

FIG. 4. **Generation of PHF-like tau filaments in cultured human neuroblastoma cells.** Tau-expressing SH-SY5Y cells were incubated for 5 days with aggregated Aβ$_{42}$ preparations, extracted with sarkosyl, and protein extracts were analyzed by immunoelectron microscopy. *A*, a typical PHF extracted from an AD brain has a width of 20 nm and a periodicity of 80 nm. *B* and *C*, tau filaments extracted from wild-type tau-expressing cells have a width of 20 nm and a periodicity of 150–160 nm. To reveal the periodicity, part of the filament in *panel C* is shown at a higher magnification in (*C′*). *D* and *E*, filaments extracted from undifferentiated P301L tau-expressing cells have a width of 20 nm and a periodicity of 130–140 nm, resembling the narrow, twisted ribbons identified in human P301L carriers. Both types of filaments are labeled with antibody Tau-5A6. *Scale bar*, 40 nm (*A–C*, *D–E*), 20 nm (*C′*).

neuronally differentiated P301L and wild-type tau-expressing cells with the phospho-Ser-422-specific antiserum pS422 and included the phospho-Ser-202/Thr-205-specific antibody AT8 as a control. 200 cells were counted for each experimental condition. Aβ$_{42}$ treatment did not cause increases in the numbers of AT8-positive cells; all HT7-positive tau-expressing cells were also AT8-positive, even in the absence of Aβ$_{42}$ (data not shown). In contrast, incubation of P301L-expressing cells with Aβ$_{42}$ for 1 day caused a more than 2-fold increase in the number of pS422-positive cells compared with HT7-positive cells, whereas wild-type tau-expressing cells required treatment for 5 days with Aβ$_{42}$ to increase the ratio of pS422-positive cells (19) (Fig. 6, *A–D*). This difference was statistically significant (*, wild-type cells treated with Aβ$_{42}$ for 5 days: 29.81% ± 7.04% pS422-positive cells/HT7-positive cells; wild-type cells treated with vehicle for 5 days: 18.75% ± 9.49%; *p* < 0.05; **, P301L cells treated with Aβ$_{42}$ for 1 day: 64.66% ± 12.93% pS422/HT7-positive cells; P301L cells treated with vehicle for 1 day: 27.93% ± 5.60%; *p* < 0.002; Mann-Whitney *U* test).

To better characterize the role of Ser-422 in tau filament formation, we mutated Ser-422 to alanine or glutamic acid and expressed either P301L/S422A or P301L/S422E double mutants both in undifferentiated and in neuronally differentiated cells at similar levels as compared with the wild-type and P301L single mutant cells (Fig. 1*A*). The Ser-422 mutations were introduced into the P301L mutant and not into the wild-type tau expression constructs because the P301L cells showed the strongest phospho-Ser-422 staining. Next, we incubated the undifferentiated cells for 5 days with Aβ$_{42}$ and fractionated tau into the RAB fraction, the RIPA-soluble fraction, and the FA-soluble fraction. In contrast to Aβ$_{42}$-treated P301L tau-expressing cells, tau was not present in the FA fraction of P301L/S422A and P301L/S422E extracts, indicating that mutagenesis of Ser-422 blocked the Aβ$_{42}$-mediated decrease in the solubility of tau (Fig. 6*E*).

TABLE I

Tau filament formation

The data were obtained after 5 days of treatment with $A\beta_{42}$ preparations.

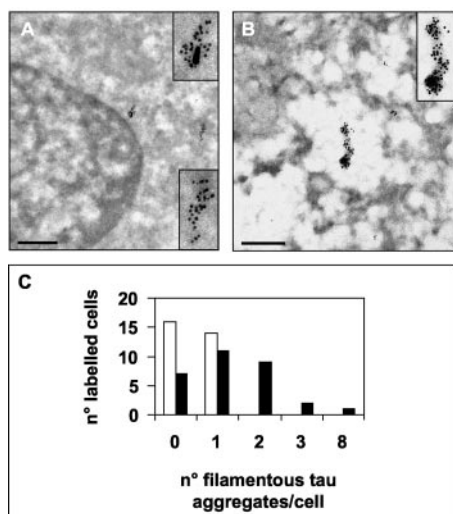|	Undifferentiated		Differentiated	
	PBS	$A\beta_{42}$	PBS	$A\beta_{42}$
Mock	ND[a]	ND	No	No
Wild-type tau	No	Yes	No	Yes
P301L tau	No	Yes	No	Yes
P301L/S422E tau	No	No	No	No
P301L/S422A tau	No	No	No	No

[a] ND, not determined

FIG. 5. **Cryoelectron microscopy of ultra-thin sections.** *A* and *B*, undifferentiated wild-type tau-expressing cells were treated with $A\beta_{42}$ for 5 days, and cryosections were obtained and incubated with the human tau-specific antibody, Tau-5A6, followed by a gold-labeled secondary antibody. Two sections obtained from $A\beta_{42}$-treated cells are shown. As controls, untreated cells were included and the primary antibody was omitted. Immunoelectron microscopy reveals many gold-decorated aggregates in the cytoplasm of neurons that were treated with $A\beta_{42}$. *C*, for a semiquantitative analysis, a cutoff of 15 gold particles was defined, and groups of gold particles were counted per cell in $A\beta_{42}$-treated (■) compared with untreated cells (□), revealing an increase in the number of filamentous tau aggregates in $A\beta_{42}$-treated cells. *Scale bar*, 300 nm (*A*), 200 nm (*B*).

Finally, we determined whether treatments with $A\beta_{42}$ would induce PHF-like tau filaments in either double mutant cell line. We did not find any evidence for PHF-like tau filament formation in the presence of the S422A or the S422E mutation (Table I). Together, these data suggest an important role of Ser-422 in $A\beta_{42}$-induced tau filament formation.

DISCUSSION

The results of this study show that $A\beta_{42}$ decreases the solubility of tau and induces PHF-like tau filaments in a human tissue culture system. A 5-day incubation with aggregated synthetic $A\beta_{42}$ of SH-SY5Y neuroblastoma cells that had been stably transfected with expression constructs encoding the longest human tau isoform, with or without the pathogenic FTDP-17 mutation P301L, caused a substantial amount of tau to appear in the FA fraction. A quantitative TaqMan PCR analysis of $A\beta_{42}$-treated cells did not reveal increased tau mRNA synthesis, although increases below 1.5-fold would not be detected by this method. Instead, the increased appearance of tau in the FA fraction indicates a role of $A\beta_{42}$ in the biophysical properties of tau that determine its solubility within cells. However, we cannot exclude that $A\beta_{42}$ may also affect the turnover rate of tau. The decreased solubility of tau in response to exposure to $A\beta_{42}$ was also associated with the formation of
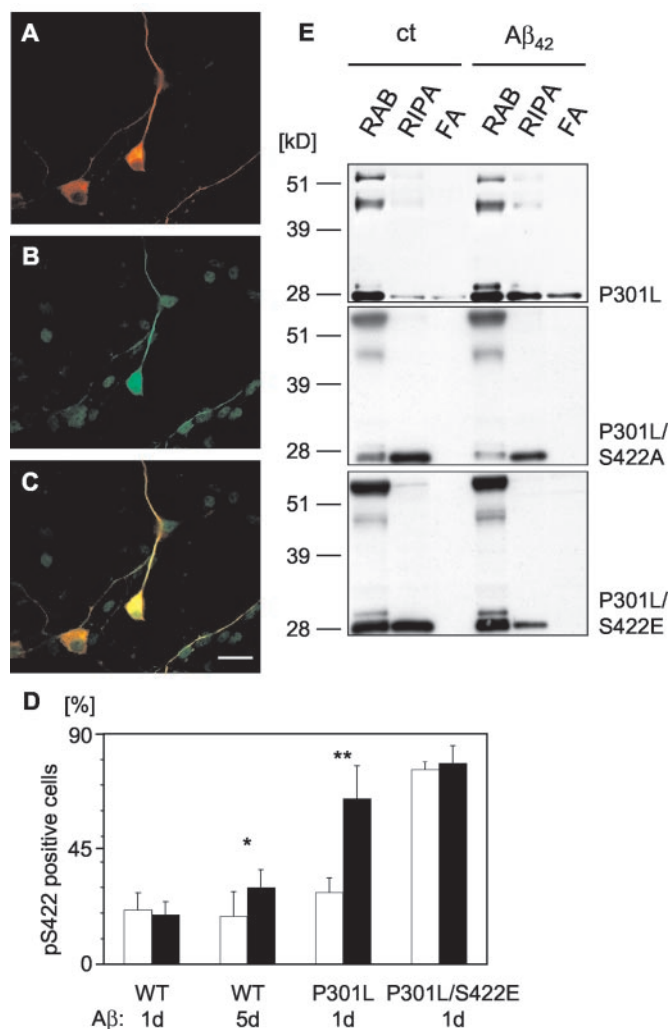

FIG. 6. **Role of the epitope Ser-422 of tau.** *A–C*, immunocytochemistry of differentiated wild-type tau-expressing cells incubated for 5 days with $A\beta_{42}$ using the human tau-specific antibody HT7 (*A*, *red*) and the pS422 antiserum specific for tau phosphorylated at Ser-422 (*B*, *green*) shows the distribution of phosphorylated tau relative to total tau (*C*, *merge*). *D*, wild-type tau-expressing cells require a treatment for 5 days with $A\beta_{42}$ (■) to increase the ratio of pS422-positive cells relative to total tau-expressing, HT7-positive cells compared with vehicle-treated cells (□). In contrast, incubation of P301L-expressing cells with $A\beta_{42}$ for 1 day already causes a more than 2-fold increase in the number of pS422-positive cells. 200 cells were counted for each experimental condition. Mann-Whitney *U* test: *, $p < 0.05$ comparing $A\beta_{42}$-treated wild-type cells with vehicle-treated wild-type cells, and **, $p < 0.002$ comparing $A\beta_{42}$-treated P301L cells with vehicle-treated P301L cells. The AT8 antibody directed against phosphorylated Ser-202/Thr-205 stains all HT7-positive cells, irrespective of $A\beta_{42}$ treatments (data not shown). *E*, in contrast to P301L mutant tau-expressing cells, tau is not present in the FA fraction of extracts obtained from $A\beta_{42}$-treated P301L/S422A and P301L/S422E cells. *Scale bar*, 20 μm (*A–C*).

twisted tau filaments as shown by negative contrast electron microscopy of sarkosyl protein extracts. These resembled the PHF extracted from NFT in human neurodegenerative diseases and are best described as narrow twisted ribbons (17). This difference in periodicity to the PHF extracted from human postmortem brains may be related to the known influence of the ratio of 4-repeat to 3-repeat human tau. In comparison to the 1:1 ratio in human brains (4), this ratio was high (above 10:1) in our experimental system.

The ultrastructural characteristics of abnormal filaments in human neurodegenerative diseases vary with pathogenic mutations (4, 5). We found that the PHF-like filaments extracted from cells expressing P301L mutant tau had shorter periodici-

ties of 130–140 nm compared with wild-type tau filaments, consistent with the fact that mutations can affect the phenotype of the tau filaments. For comparison, the twisted ribbons in FTDP-17 patients carrying the P301L mutation have periodicities of greater than 130 nm (4), whereas the tau filaments in *Drosophila* generated by expression of human 4-repeat wild-type tau have periodicities of 45 nm (20).

Our data are consistent with our previous results of $A\beta_{42}$-induced PHF-like tau filament formation in transgenic mice (9), but in contrast to the transgenic mice $A\beta_{42}$-induced PHF formation in tissue culture also occurred with wild-type tau. This may be related to the species difference and points to the possibility that human cells in culture may be more susceptible to the formation of abnormal tau filaments as compared with murine cells *in vivo*. Fibrillar aggregates of tau were previously observed in Chinese hamster ovary cells that had been transfected with triple mutant tau expression constructs (21). In a related study (22), combined treatments of SH-SY5Y cells with okadaic acid and 4-hydroxynonenal induced 2–3-nm-wide fibrillar tau polymers. The PHF-like filaments in our tissue culture system clearly differed from both of the above in that they were much longer, about 10 times wider, and had readily identifiable twisted structures (Fig. 4). This difference could well be related to the prolonged exposure to $A\beta_{42}$ in our experiments, because we could not observe any filamentous structures for up to 2 days of exposure to $A\beta_{42}$ (Table I).

A semi-quantitative analysis of filament analysis by immunoelectron microscopy on ultra-thin cryosections of cells revealed a significant increase in the number of tau aggregates in $A\beta_{42}$-treated cells. The albeit-low number of aggregates in the untreated group is not unexpected, because overexpression of tau in itself is likely to cause some aggregation as has been shown *in vivo* for wild-type or P301L mutant tau-expressing mice in the absence of $A\beta_{42}$ (6, 7, 23).

The expression of P301L mutant tau in transgenic mice showed that the presence of a pathogenic mutation is required for both early and substantial tau filament and tangle formation; wild-type tau transgenic mice develop only a few tangles at very old age, despite higher expression levels of the transgene (7, 24). Obviously, in mice, the pathogenic mutation is needed to catalyze the pathogenic conversion of tau, which is not the case in our cellular model. Therefore, our cellular model mimics more closely human sporadic AD, where tau filament formation occurs in the absence of tau mutations and tau overexpression. However, it has to be kept in mind that in humans AD needs decades to develop, whereas *in vitro* pathological changes have to be achieved within a few days or *in vivo* within a few months, asking for high (and therefore unphysiological) levels of tau expression.

Our data also imply that either the Ser-422 site of tau itself or its phosphorylation are necessary, although not sufficient, for tau filament formation. Despite the presence of the P301L mutation that in humans and in tau transgenic mouse models enhances tau filament formation, the S422A and S422E mutants did not form tau filaments by incubating the cells with $A\beta_{42}$. In transgenic mice expressing P301L tau, Ser-422, but not the AT8 epitope Ser-202/Thr-205, was among the epitopes that were selectively phosphorylated in response to $A\beta_{42}$ injections (9). $A\beta_{42}$ treatment did not cause increases in the numbers of AT8-positive cells because all HT7-positive tau-expressing cells were also AT8-positive, even in the absence of $A\beta_{42}$. These findings are in agreement with those obtained in mice (9). In contrast, incubation of P301L-expressing cells with $A\beta_{42}$ for only 1 day caused a more than 2-fold increase in the number of pS422-positive cells compared with HT7-positive cells.

Mutagenesis of Ser-422 revealed that tau was not present in the FA fraction of $A\beta_{42}$-treated P301L/S422A or P301L/S422E cells, in contrast to $A\beta_{42}$-treated wild-type or P301L tau-expressing cells. Similarly, we did not find any evidence for PHF-like tau filament formation in the presence of the S422A or the S422E mutation, suggesting an important role of Ser-422 both in the $A\beta_{42}$-induced decrease in tau solubility and in tau filament formation (Table I). The finding that mutating the serine of epitope 422 to glutamic acid also precluded tau filament formation was unexpected because the S422E modification was designed to mimic the negative charge caused by phosphorylation of this site. Thus, the sole addition of a negative charge at this site is not sufficient to induce the formation of PHF-like tau filaments; coordinated phosphorylation at multiple residues, including Ser-422, may be required. Tau adopts distinct conformations during sequential phosphorylation reactions, and the AD-specific phosphoepitope AT100 can only be generated by a sequential phosphorylation of tau, initially by glycogen synthase kinase-3β followed by protein kinase A, indicating that prephosphorylation at particular sites can alter the conformation and prevent phosphorylation at other sites (25). An alternative explanation is provided by the fact that Ser-422 is located next to a putative caspase-3 cleavage site at position 421 and that altered caspase cleavage is involved in the rates of filament formation (26–28).

CONCLUSION

In conclusion, we established a tissue culture system for the generation of *bona fide* PHF-like filaments that closely resembled those extracted from brains of AD patients. The results provided by this system are compatible with an important role of $A\beta_{42}$ in the generation of NFT in AD, and with a pivotal, yet not exclusive, role of the Ser-422 epitope of tau in tau fibrillogenesis. Our data imply that either the Ser-422 site itself or its phosphorylation are necessary, but not sufficient, for tau filament formation. PHF-like tau filament formation was achieved within 5 days, much faster than in current transgenic mouse models (8, 9). Therefore, this culture system will be useful to map phosphoepitopes of tau involved in PHF formation and to identify and characterize modifiers of the tau pathology. Further adaptation of the system may allow the screening and validation of compounds designed to prevent PHF formation.

REFERENCES

1. Hutton, M., Lendon, C. L., Rizzu, P., Baker, M., Froelich, S., Houlden, H., Pickering-Brown, S., Chakraverty, S., Isaacs, A., Grover, A., Hackett, J., Adamson, J., Lincoln, S., Dickson, D., Davies, P., Petersen, R. C., Stevens, M., de Graaff, E., Wauters, E., van Baren, J., Hillebrand, M., Joosse, M., Kwon, J. M., Nowotny, P., Heutink, P., *et al*. (1998) *Nature* **393,** 702–705
2. Poorkaj, P., Bird, T. D., Wijsman, E., Nemens, E., Garruto, R. M., Anderson, L., Andreadis, A., Wiederholt, W. C., Raskind, M., and Schellenberg, G. D. (1998) *Ann. Neurol.* **43,** 815–825
3. Spillantini, M. G., Murrell, J. R., Goedert, M., Farlow, M. R., Klug, A., and Ghetti, B. (1998) *Proc. Natl. Acad. Sci. U. S. A.* **95,** 7737–7741
4. Lee, V. M., Goedert, M., and Trojanowski, J. Q. (2001) *Annu. Rev. Neurosci.* **24,** 1121–1159
5. Gotz, J. (2001) *Brain Res. Brain Res. Rev.* **35,** (suppl.) 266–286
6. Lewis, J., McGowan, E., Rockwood, J., Melrose, H., Nacharaju, P., Van Slegtenhorst, M., Gwinn-Hardy, K., Murphy, M. P., Baker, M., Yu, X., Duff, K., Hardy, J., Corral, A., Lin, W. L., Yen, S. H., Dickson, D. W., Davies, P., and Hutton, M. (2000) *Nat. Genet.* **25,** 402–405
7. Gotz, J., Chen, F., Barmettler, R., and Nitsch, R. M. (2001) *J. Biol. Chem.* **276,** 529–534
8. Lewis, J., Dickson, D. W., Lin, W.-L., Chisholm, L., Corral, A., Jones, G., Yen, S.-H., Sahara, N., Skipper, L., Yager, D., Eckman, C., Hardy, J., Hutton, M., and McGowan, E. (2001) *Science* **293,** 1487–1491

9. Gotz, J., Chen, F., van Dorpe, J., and Nitsch, R. M. (2001) *Science* **293,** 1491–1495

10. Encinas, M., Iglesias, M., Liu, Y., Wang, H., Muhaisen, A., Cena, V., Gallego, C., and Comella, J. X. (2000) *J. Neurochem.* **75,** 991–1003

11. Hartley, D. M., Walsh, D. M., Ye, C. P., Diehl, T., Vasquez, S., Vassilev, P. M., Teplow, D. B., and Selkoe, D. J. (1999) *J. Neurosci.* **19,** 8876–8884

12. Johnson, G. V., Seubert, P., Cox, T. M., Motter, R., Brown, J. P., and Galasko, D. (1997) *J. Neurochem.* **68,** 430–433

13. Bussiere, T., Hof, P. R., Mailliot, C., Brown, C. D., Caillet-Boudin, M. L., Perl, D. P., Buee, L., and Delacourte, A. (1999) *Acta Neuropathol.* **97,** 221–230

14. Probst, A., Gotz, J., Wiederhold, K. H., Tolnay, M., Mistl, C., Jaton, A. L., Hong, M., Ishihara, T., Lee, V. M., Trojanowski, J. Q., Jakes, R., Crowther, R. A., Spillantini, M. G., Burki, K., and Goedert, M. (2000) *Acta Neuropathol.* **99,** 469–481

15. Goedert, M., Spillantini, M. G., Cairns, N. J., and Crowther, R. A. (1992) *Neuron* **8,** 159–168

16. Crowther, R. A. (1991) *Proc. Natl. Acad. Sci. U. S. A.* **88,** 2288–2292

17. Spillantini, M. G., Crowther, R. A., Kamphorst, W., Heutink, P., and van Swieten, J. C. (1998) *Am. J. Pathol.* **153,** 1359–1363

18. Uberti, D., Rizzini, C., Spano, P. F., and Memo, M. (1997) *Neurosci. Lett.* **235,** 149–153

19. Haque, N., Tanaka, T., Iqbal, K., and Grundke-Iqbal, I. (1999) *Brain Res.* **838,** 69–77

20. Jackson, G. R., Wiedau-Pazos, M., Sang, T.-K., Wagle, N., Brown, C. A., Massachi, S., and Geschwind, D. H. (2002) *Neuron* **34,** 509–519

21. Vogelsberg-Ragaglia, V., Bruce, J., Richter-Landsberg, C., Zhang, B., Hong, M., Trojanowski, J. Q., and Lee, V. M. (2000) *Mol. Biol. Cell* **11,** 4093–4104

22. Perez, M., Hernandez, F., Gomez-Ramos, A., Smith, M., Perry, G., and Avila, J. (2002) *Eur. J. Biochem.* **269,** 1484–1489

23. Ishihara, T., Zhang, B., Higuchi, M., Yoshiyama, Y., Trojanowski, J. Q., and Lee, V. M. (2001) *Am. J. Pathol.* **158,** 555–562

24. Ishihara, T., Hong, M., Zhang, B., Nakagawa, Y., Lee, M. K., Trojanowski, J. Q., and Lee, V. M. (1999) *Neuron* **24,** 751–762

25. Zheng-Fischhofer, Q., Biernat, J., Mandelkow, E. M., Illenberger, S., Godemann, R., and Mandelkow, E. (1998) *Eur. J. Biochem.* **252,** 542–552

26. Abraha, A., Ghoshal, N., Gamblin, T. C., Cryns, V., Berry, R. W., Kuret, J., and Binder, L. I. (2000) *J. Cell Sci.* **113,** 3737–3745

27. Fasulo, L., Ugolini, G., Visintin, M., Bradbury, A., Brancolini, C., Verzillo, V., Novak, M., and Cattaneo, A. (2000) *J. Neurochem.* **75,** 624–633

28. Berry, R. W., Abraha, A., Lagalwar, S., LaPointe, N., Gamblin, T. C., Cryns, V. L., and Binder, L. I. (2003) *Biochemistry* **42,** 8325–8331

β-Amyloid Induces Paired Helical Filament-like Tau Filaments in Tissue Culture

Alessandra Ferrari, Frederic Hoerndli, Thomas Baechi, Roger M. Nitsch and Jürgen Götz

Access the most updated version of this article at doi: 10.1074/jbc.M308243200